Correlated MO Study of the Low-Barrier Intramolecular Motions in Donor−Acceptor Ethenes

Snezhana M. Bakalova,[†] Luis Manuel Frutos,[‡] Jose Kaneti,*[,†,‡] and Obis Castaño[‡]

Institute of Organic Chemistry with Centre of Phytochemistry, Bulgarian Academy of Sciences, 1113 Sofia, Bulgaria, and Department of Physical Chemistry, University of Alcalá, 28871 Alcalá de Henares, Madrid, Spain

Received: April 11, 2005; In Final Form: September 13, 2005

Correlated MP2 and MCSCF MO calculations of several model push−pull ethenes in most cases indicate no great participation of excited singlet and triplet electronic configurations in either the minima or the transition structures for the suggested facilitated intramolecular rotation about the polarized C═C bond. This situation changes significantly only in molecules with sulfur atoms in the molecule as either donors or acceptors. The outstanding contribution of sulfur atoms as either donors or acceptors is a significant increase of push−pull ethene molecular polarizabilities. Thus, within the studied small series of mostly planar push−pull ethenes, polarizability appears a better indicator of rapid intramolecular motions about the C═C bond than straight polarity. Substituents with larger steric demands around the C═C bond are shown to likely preclude its complete turnaround, thus prompting a ramification of the interpretations of dynamic NMR phenomena in sterically constrained push−pull ethenes as large-amplitude librations resulting from strong rovibrational and relatively weak electronic coupling. These librations, as shown by complete vibrational mode analysis of corresponding rotational transition structures, cover in fact certain sectors of the intuitively suggested full rotations similar to those about C−C single bonds.

Introduction

Photochemical and photophysical processes in substituted ethenes are inseparable from the notion of S−T intersystem crossings or S−S, respectively, T−T conical intersections, frequently observed processes usually initiated by ultraviolet or visible light. In fact, all photoreactions of ene systems having the characteristic C═C type of bonding, and leading to stable products, necessarily occur via crossings between two electronic potential energy surfaces.[1] With substituted ethenes, this is most frequently a singlet−triplet crossing and is closely related to their cis−trans photoisomerization. The involvement of a triplet, though, is not a necessary element of ethene or polyene cis−trans isomerization.[1] Whatever the specific mechanism of a given ethene cis−trans isomerization, the process is formally equivalent to a twist of the usually rigid C═C bond, and thus to a conformational isomerization. The experimentally established barriers to such processes are usually higher than 65 kcal·mol^{-1}.

Ethenes of type **1**, where D is for (π-)donor and A for (π-)acceptor, are strongly polarized in their ground electronic states.[2] The D^+A^- polarization can bring about quite a significant extension of the originally short C═C bond, which could consequently lead to a remarkable—more than 20 kcal·mol^{-1}—lowering of the usually high barriers to rotation about C═C bonds,[3] so that the corresponding dynamic processes would be observable by NMR.[4] However, registered experimental barriers depend significantly on the choice of model compounds. NMR dynamic phenomena in molecules with relatively rigid donor fragments, e.g. in the presence of aromatic or unsaturated heterocyclic subunits,[5−7] are simpler to interpret than those of saturated donor heterocycles[6] **2**−**5** or presumably freely rotating and inverting compounds such as **6**.[8] More sophisticated temperature-dependent dynamics[3,5,6,9] and 2-D NMR experiments[10−12] in solution also register the occurrence of relatively low barrier processes for compounds **2**−**6**, which have routinely been interpreted as significantly easier twisting of the polarized C═C bond.[13] The corresponding thermodynamic barriers are dependent on D and A substituents, respectively,[5−7,9,15,16] as well as on the polarity of solvents,[5,6,9] which is understood as corroboration of their interpretation as rotations around the polarized C═C bond.

The barriers obtained by the mentioned NMR methods[5−12] for model compounds of types **2** and **3** are in the range of 12−23 kcal·mol^{-1}. However, the theoretical DFT C═C rotational barriers of push−pull ethenes **1** span the range between 7 and more than 30 kcal·mol^{-1}.[13,16] While the theoretically found upper limit is obviously somewhat beyond the notion of free intramolecular rotation, the lower limit certainly deserves special attention. The significant contribution of single-bonded polar electronic configurations $D_2C^+-C^-A_2$ to the ground states of push−pull ethenes **1** has attracted notable theoretical attention.[5−7,9,14−16] However, most authors have avoided discussion of possibilities for the indicated intersystem crossing, prudently leaving the problem to multiconfigurational MO calculations.[3,17] Internal rotation around the C═C bond should result in loss of double bond character, and theoretical calculation of acceptable rotational barriers by single-configurational methods as HF theory would be reliable only in the case of favorable cancellation of correlation effects in the relevant ground and transition structures.[18] In addition, polarized double bonds in push−pull ethenes have significant zwitterionic character even in the

* Corresponding author.
[†] Bulgarian Academy of Sciences.
[‡] University of Alcalá.

10.1021/jp051864f CCC: $30.25
Published on Web 10/26/2005

SCHEME 1: Model Push−Pull Ethenes Subjected to the Correlated Calculations

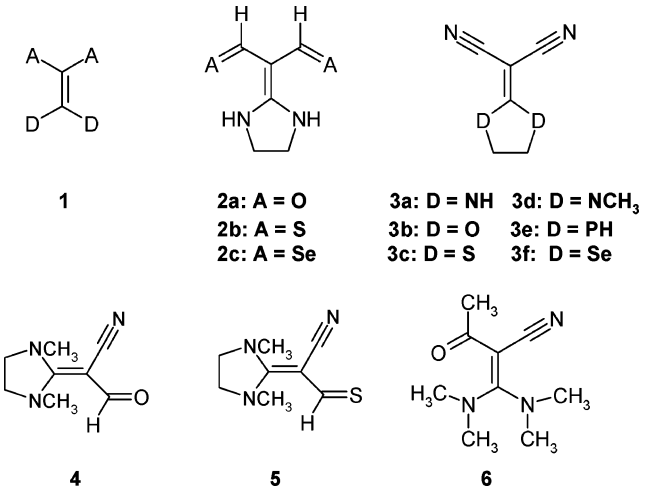

supposedly planar conformational minimum. Therefore, contributions of excited singlet and/or triplet electronic configurations to the C═C rotational transition structure of push−pull ethenes are usually considered negligible. However, precise localization of rotational transition structures of push−pull ethenes by Hartree−Fock (HF), second order Møller−Plesset (MP2), and even density functional theory (DFT) methods often fails,[5,14,15] which has been attributed to instability of both DFT and MP2 results with respect to singlet−triplet contamination.[3,19] These circumstances have stimulated our interest to study explicitly the contribution of singlet and triplet electronic configurations to the C═C internal rotation in push−pull ethenes in more detail than has been attempted recently.[3,5,14,15,17] For the sake of comparison with earlier calculations at other levels of theory, as well as with experimental results, our choice of model molecules has been limited to compounds **2**−**6**, as shown in Scheme 1 and Tables 1 and 2. The majority of cyclic model compounds **2** and **3** of the above series have been extensively studied both experimentally and theoretically,[6] showing relatively low C═C rotation barriers. It should be noted, however, that significant participation of triplet electronic configurations in the C═C rotation TS has normally been associated with high rotational barriers,[5,7] which is another problem in need of clarification.

An initial crude estimate of singlet and triplet conformational energy profiles for the C═C rotation in compounds **2a**,**b**, and **3a**−**d**, respectively, can be obtained by a relaxed scan of the respective energy surface at the ROHF/6-31G* level. However, a better account for electron correlation effects along the surmised internal rotation path can be achieved by (U)DFT and/or (U)MP2 calculations. We have selected the MP2 (frozen core) approach, being indeed aware of the possible significant spin contamination of the open shell solutions. A reliable remedy to this, as has been noted much earlier,[17,19] are MCSCF (CAS SCF) calculations,[20−22] which produce spin states uncontaminated by wave functions of higher multiplicity and can thus allow explicit determination of the extent of electronic state interactions in the selected push−pull ethenes. These types of calculations should also clarify the possible involvement of intersystem crossings in the twistings of strongly polarized C═C bonds.

Computational Details

Single-determinant wave functions, that is, ROHF and MP2 calculations in this work, use the GAUSSIAN 03 program package,[23] which is used also in the search of potential surface $S_m - S_n$, $m \neq n$, conical intersections or of S−T intersystem crossings of electronic states.[22] Multiconfigurational MCSCF and MC-QDPT2[24] calculations are done with GAMESS-US.[25] Selected active configuration spaces involve preferentially some of the frontier π-orbitals of studied molecules: eight electrons in eight orbitals.[20] Full geometry optimizations are carried out at ROHF/6-31G* and MP2/6-31G* levels, as well as at the 8 × 8 MCSCF/6-31G* level. Stationary structures, e.g. minima and TS, are verified by calculations of analytical vibrational frequencies at the MP2/6-31G* level.[26] This complete vibrational analysis provides the requisite transition vectors of corresponding unique imaginary vibrational modes of the located TS as well as the visual mechanistic description of associated intramolecular motions. In the cases of fully optimized minima, vibrational analysis of the low-frequency real modes gives the basis of proposed refinements to the interpretation of the observed NMR dynamic phenomena.

As dictated by available computational resources, the active correlation space for the MCSCF and MC-QDPT2/6-31G* calculations is chosen to cover the eight π-electrons in occupied MO's and spanning four occupied and four virtual π-orbitals in **2a**, **3a**, **3b**, and **3d**.[20] For consistency, with the sulfur compounds **2b** and **3c** we use active spaces of the same size, even though their two higher virtual MO's are sulfur σ-MO's.[20] No vibrational frequency calculations are done at the MCSCF level due to unavailable analytical second energy derivatives.

Optimizations at the 8 × 8 MCSCF/6-31G* level with eight electrons in eight active orbitals do not bring significant geometry changes with respect to MP2/6-31G* geometries. Therefore, single-point 8 × 8 MC-QDPT2 calculations[24,25] at the correlation-consistent cc-pVTZ basis set level[27] are used to refine the results of lower theoretical level calculations. To reduce the vast memory requirements and the necessary huge scratch disk space in MCSCF and MC-QDPT2 calculations, the cc-pVTZ basis set has been truncated of f-functions on nonhydrogen atoms, as well as of d-functions on H, thus becoming a [10s5p2d − 4s3p2d] for C, N, O; [5s2p − 3s2p] for H; and [15s9p2d − 5s4p2d] for S. This truncation of cc-pVTZ basis set expansions considerably improves the MCSCF convergence as well.

Spin−orbit couplings between S_0 and T_1 electronic states are calculated using the full Breit−Pauli electronic transition Hamiltonian,[28,29] as implemented in GAMESS-US.[25] Structures, orbitals, and vibrational modes are visualized and plotted using MOLDEN[30] and GaussView.[23]

Results and Discussion

Computed energies of push−pull ethene models **2** and **3** at the various MO theory levels are summarized in Table 1. The rotational barriers, calculated at our highest level, 8 × 8 MC-QDPT2/cc-pVTZ//MP2/6-31G*, with ΔG Gibbs energy corrections at 300 K from MP2/6-31G* calculations, are listed in Table 2.

Structural Details. Earlier theoretical studies indicate significant variations of the electronic structure of push−pull ethenes, depending on the specific interactions in any particular combination of D and A. For example, the computed length of the C═C bond varies within a 1.35−1.45 Å range at the HF/6-31G* level and is definitely related to C═C bond polarization,[6] at least for first row D and A atoms. The registered barriers $\Delta G^{\ddagger}$ of dynamic processes, interpereted as C═C rotations, also correlate fairly well with quantities such as $\Delta\delta_{C=C}$,

TABLE 1: MO Computational Results—ROHF,[20] MP2,[20] and CAS[20,22] [a]

compd	ROHF S_0 TS rot. ΔE	CAS min S_0 CAS‡ S_0 singlet ΔE $\Delta\Delta G^{\ddagger}$	MP2/6-31G* $E + \Delta G$ α_{xx}	MP2/6-31G*‡ $E + \Delta G$ rot. $\Delta\Delta G^{\ddagger}$	RHF (ref 6)
2a	−490.496 90	−490.605 35	−491.925 82	−491.880 35	
	−490.456 64	−490.565 63	−491.813 82	−491.769 89	
	$\Delta E = 25.2$	$\Delta E = 24.9$	109.5	$\Delta\Delta G = 27.6$	$\Delta E = 25.8$
		23.9			
2b	−1130.191 61	−1135.860 11	−1137.099 33	−1137.070 49	
	−1130.171 84	−1135.826 90	−1136.993 75	−1136.965 62	
	$\Delta E = 12.4$	$\Delta E = 20.8$	207.5	$\Delta\Delta G = 17.7$	$\Delta E = 10.9$
		20.4			
2c		−5136.042 13	−5137.203 84	−5137.180 20	
		−5136.019 56	−5137.102 36	−5137.081 19	
		$\Delta E = 14.2$	249.5	$\Delta\Delta G = 13.3$	
		12.7			
3a	−448.483 76	−448.627 07	−449.869 67	−449.823 86	
	−448.441 25	−448.590 35	−449.782 09	−449.735 35	
	$\Delta E = 26.7$	$\Delta E = 23.0$	41.9	$\Delta\Delta G = 29.3$	$\Delta E = 27.2$
		23.6			
3b	−488.121 09	−488.266 90	−489.532 32	−489.465 49	
	−488.060 56	−488.208 62	−489.470 50	−489.406 35	
	$\Delta E = 38.0$	$\Delta E = 36.6$	104.2*	$\Delta\Delta G = 40.3$	$\Delta E = 39.4$
		38.3			
3c	−1133.417 09	−1133.462 64	−1134.750 05	−1134.671 20	
	−1133.344 17	−1133.427 42	−1134.696 45	−1134.618 44	
	$\Delta E = 45.8$	$\Delta E = 22.1$	144.4	$\Delta\Delta G = 49.0$	$\Delta E = 49.1$
		21.6			
3d	−526.528 66	−526.681 67	−528.181 16	−528.160 09	
	−526.508 16	−526.630 15	−528.039 81	−528.017 51	
	$\Delta E = 12.9$	$\Delta E = 32.3$	134.2*	$\Delta\Delta G = 14.0$	
		33.1			
3e		−1021.071 24	−1022.278 56	−1022.170 43	
		−1020.962 55	−1022.208 67	−1022.102 63	
		$\Delta E = 68.2$	143.239*	$\Delta\Delta G = 66.5$	
3f		−5133.699 74	−5134.862 12	−5134.778 63	
		−5133.618 07	−5134.813 51	−5134.730 75	
		$\Delta E = 51.2$	137.290*	$\Delta\Delta G = 51.9$	

[a] Active CAS configuration spaces are 8 × 8; the basis set is 6-31G*.[13] Absolute energies are given in atomic units, and ΔE, $\Delta\Delta G^{\ddagger}$ (barriers to C═C rotation) are in kilocalories per mole. $\Delta G^{\ddagger}$ corrections at the MP2/6-31G* level are used at the 8 × 8 MC SCF/6-31G* level as well. *α_{zz} = the largest component of the polarizability tensor; **single-point 8 × 8 MCSCF/6-31G*//MP2/6-31G* calculations.

the difference of ^{13}C chemical shifts of ethene carbon atoms, which characterize the push−pull effect experimentally.[28] However, both HF and MP2 computational models have been reported to systematically overestimate the experimental NMR barriers.[6] Estimates of C═C rotation barriers from B3LYP/6-31G* calculations[13] are apparently closer to the experimental values.

The so far most extensive comparison of experimental NMR data and theoretical results from MO calculations[6] relies on geometries, optimized at the HF/6-31G* level. Reported rotational minima around the C═C bond are strictly planar, while in the rotation transition structures the planes of donor atoms are perpendicular to those of acceptor atoms.[6] However, reoptimization of geometries of model compounds **2** and **3** shows at even the ROHF/6-31G* level a certain degree of pyramidality of donor heteroatoms in the five-membered rings. At the MP2/6-31G* level, planar structures are in fact transition structures for a ring puckering, which is either the symmetric mode with D = NH, **3a**, or the antisymmetric one with D = O, S; **3b** and **3c** with respect to the C═C 2-fold axis. With D = NCH_3, **3d**, these ring puckering vibrations are two of A_2, and one of B_1 symmetry. In the case of N donors, **3a**, **3d**, **4**−**6**, the B_1 vibration effectively brings about a carbon pyramidalization at the donor end of the C═C bond as well. With O and S donors, **3b**, and **3c**, the A_2 ring puckering vibrations are effectively equivalent to C═C bond twisting, which is the "C═C rotation" searched for, and requires indeed a significantly lower barrier to the process than the "genuine" rotation with the TS having perpendicular planes of donor and acceptor substituents, including the corresponding carbon atom of the formal polarized double bond. Therefore, tightly optimized ground electronic state structures **2** and **3** with no symmetry constraints have slightly twisted heterocyclic rings of C_2 symmetry instead of C_{2v} at the HF/6-31G*, as well as at the MP2/6-31G(d) computational level, Figure 1. Similarly, all atoms around the formal double bond in "truly perpendicular" C═C rotational transition structures are more or less pyramidal, Figure 1. For these reasons we have to reconsider the electronic structure changes along the suggested C═C bond rotation at higher theoretical levels than those used so far.[5,6,10] Throughout these calculations, the MP2/6-31G* vibrational analysis is our best level to obtain the necessary thermodynamic contributions to the total energy which provide the required estimates of measurable barriers of unhindered full rotations (irrespective of whether coupled with other vibrational modes or not) about the polarized C═C bonds. Note that the lowest frequency vibrational mode of ground rotational states of studied push−pull ethenes is the C═C twisting mode, i.e., the suggested C═C rotation, strongly coupled with heteroatom inversions, Figure 2. This mode is preserved as the transition mode in the rotational TS's. The conservation of the coupled internal rotation−inversion vibrational mode in both the fully relaxed rotational minimum and in the corresponding transition structure for the rotational isomerization is the necessary and sufficient guarantee for the correct assignment of the considered

TABLE 2: Calculated MP2/6-31G*, (8×8)MC-SCF/6-31G*// (8×8)MC-SCF/6-31G*, and (8×8)MC-QDPT2/cc-pVTZ// MP2/6-31G* Energies (au) and Rotation Barriers Thereof[a]

Compound		MP2	NImag v, cm^{-1}	$R_{C=C}$	MP2 +ΔG	8x8 CAS	MC-QDPT2
2a	S_0	-491.92582	0	1.411	-491.81382	-490.76901	-492.32607
TS – S		-491.88035	1 -90.6	1.448	-491.76989	-490.70482	-492.29696
		ΔE=28.5			ΔΔG=27.5	ΔΔG=39.3	ΔΔG=17.3
2b	S_0	-1137.09933	0	1.438	-1136.99375	-1136.02477	-1137.50803
TS – S		-1137.07335	1 -125.7	1.462	-1136.96562	-1136.00368	-1137.48257
		ΔE=16.3			ΔΔG=17.6	ΔΔG=14.5	ΔΔG=17.3
2c	S_0	-5137.20384	0	1.441	-5137.10236	-5133.69974	-5134.91088
TS – S		-5137.18020	1 -139.5	1.466	-5137.08119	-5133.61807	-5134.84050
		ΔE= 14.8			ΔΔG=13.3	ΔΔG=49.7	ΔΔG=42.7
3a	S_0	-449.86967	0	1.382	-449.78209	-448.69362	-450.19723
TS – S		-449.82386	1 -144.1	1.446	-449.73535	-448.67749	-450.16969
		ΔE=28.7			ΔΔG=29.3	ΔΔG=10.7	ΔΔG=17.9
3b	S_0	-489.53232	0	1.363	-489.46848	-488.35097	-489.89435
TS – S		-489.46549	1 -228.3	1.423	-489.40635	-488.34386	-489.84747
		ΔE=41.9			ΔΔG=39.0	ΔΔG=3.6	ΔΔG=25.5
3c	S_0	-1134.75006	0	1.371	-1134.69645	-1133.68543	-1135.11584
TS – S		-1134.67120	1 -300.3	1.441	-1134.61844	-1133.57293	-1135.03670
		ΔE=49.5			ΔΔG=49.0	ΔΔG=70.1	ΔΔG=49.1
3d plan.	S_0	-528.18116	3 -238.6	1.398	-528.03983	-526.68167	-528.59903
nonplan.	S_0	-528.18931	0	1.392			
TS – S		-528.16038	1 -101.5	1.448	-528.01751	-526.64760	-528.58495
		ΔE=18.5			ΔΔG=14.0	ΔΔG=22.4	ΔΔG=9.8
3e	S_0	-1022.27856	0	1.365	-1022.20867	-1021.07124	-1022.26671
TS – S		-1022.17043	1 -715.2	1.462	-1022.10262	-1020.96255	-1022.17086
		ΔE=67.9			ΔΔG=66.5	ΔΔG=66.7	ΔΔG=58.7
3f	S_0	-5134.86212	0	1.369	-5134.81351	-5133.69974	-5134.91088
TS – S		-5134.77863	1 -268.3	1.441	-5134.73075	-5133.61807	-5134.84050
		ΔE=52.4			ΔΔG=51.9	ΔΔG=50.7	ΔΔG=43.7
							
4	S_0	-549.20199	0	1.399	-549.04970	-547.65507	-549.66736
TS – S		-549.18181	1 -107.9	1.446	-549.02977	-547.62457	-549.64314
		ΔE=12.7			ΔΔG=12.5	ΔΔG=18.9	ΔΔG=15.0
							
5	S_0	-871.79444	0	1.405	-871.64434	-870.24045	-872.24118
TS - S		-871.77722	1 -91.7	1.453	-871.62804	-870.22633	-872.21798
		ΔE=10.8			ΔΔG=10.2	ΔΔG=8.3	ΔΔG=14.0
							
6	S_0	-589.54652	0	1.403	-589.34644	-587.78071	-589.69730
TS - S		-589.50049	1 -55.3	1.456	-589.29998	-587.75495	-589.65269
		ΔE=28.9			ΔΔG=29.2	ΔΔG=16.5	ΔΔG=28.3
							
7	S_0	-524.53469	0	1.343	-524.46462	-523.05691*	-524.89097*
TS - S		-524.45888	1 -37.4	1.411	-524.39017	-522.84998*	-524.40680*
		ΔE=47.6			ΔΔG=46.7	ΔΔG=129.0	ΔΔG=296.6
							
8	S_0	-526.96986	0	1.345	-526.84871	-525.53888*	-527.36744*
TS - S		-526.83958	1 -378.0	1.438	-526.72113	-525.22704*	-526.83453*
		ΔE=81.8			ΔΔG=80.1	ΔΔG=194.0	ΔΔG=333.7

[a] Free energies at the MC levels are calculated using the MP2 thermal corrections at 298 K. C═C rotation barriers ΔE and $\Delta G^{\ddagger}$ are given in kilocalories per mole. *(12×8)MCSCF/6-31G* and (12×8)MC-QDPT2/6-31G* calculations, respectively.

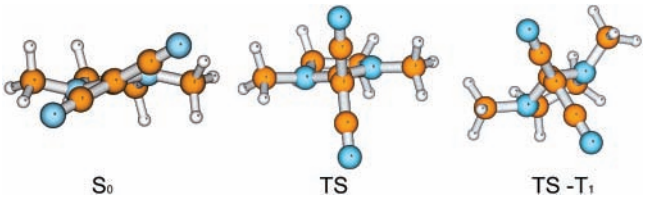

Figure 1. Optimized 8 × 8 MCSCF/6-31G(d) geometries of **3d**, left to right: S_0; the rotational transition structure of S_0; and the rotational transition structure of T_1.

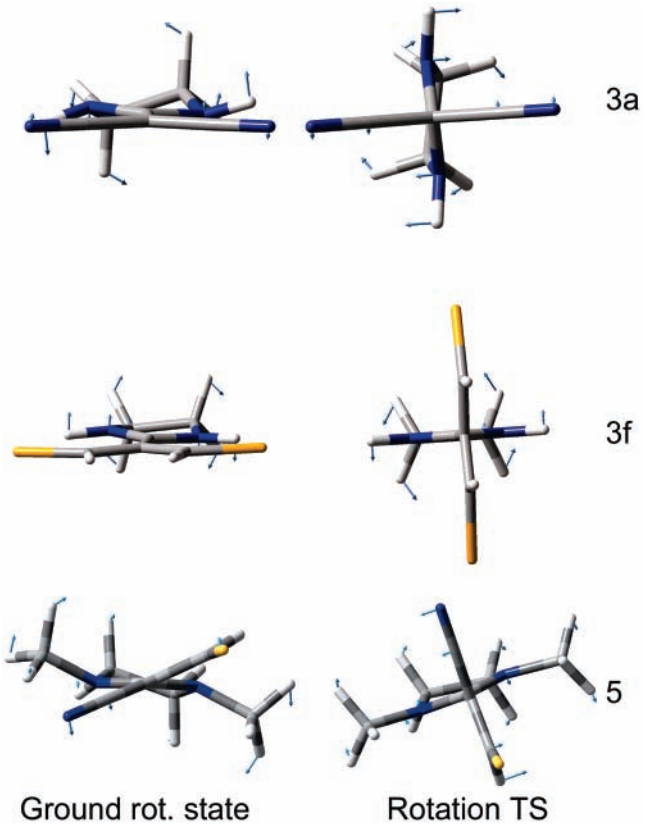

Figure 2. Lowest vibrational modes of **3a**, **3f**, and **5** at the ground state, and their rotational transition modes (compare also to Figure 1, **3d**).

molecular modes as well as of the located stationary points of the corresponding molecular potential energy surface.

Reoptimization of push−pull ethene models at the MCSCF/6-31G* level requires the selection of a sufficiently large active space,[17] which should be both computationally feasible and adequately accommodate important MO's participating in the C═C rotation. For first row elements, these can be safely assumed to be the several frontier π-orbitals, four occupied and four virtual.[17] The 8 × 8 MCSCF/6-31G* geometry optimizations of **2** and **3** series of molecules indicate planar or almost planar singlet ground-state geometries. As calculations of numerical vibrational frequencies for our models at this level are hardly feasible, we interpret the planarity of five-membered donor heterocycles at the 8 × 8 MCSCF level as an indication that corresponding MP2 calculations possibly underestimate ring puckering barriers. The same applies also to heteroatom (N, O, S) inversion barriers, though possibly with some degree of reserve. Nevertheless, our MCSCF results indeed support the selection of "planar" five-membered heterocyclic rings at the donor end of push−pull ethenes as a good means to obtain theoretical estimates of C═C rotation barriers with little if any

contribution of concomitant intramolecular motions.[6] Consequently, the 8 × 8 MCSCF calculations with the 6-31G* basis locate perpendicular rotational transition structures such as the MP2/6-31G* ones.

At the MP2/6-31G* level, the lowest electronic state of the perpendicular rotational transition structure is a singlet and is indeed the pure rotational TS, as identified by vibrational mode analysis. The ground electronic states of 8 × 8 MCSCF/6-31G* perpendicular structures are triplets, and most likely minima. In the case of **3d**, however, the perpendicular MP2/6-31G* structure has three imaginary frequencies, and the rotational mode in the lower two of these is associated with N heteroatom inversion modes; see Figures 1 and 2. Similarly, the single rotational mode in **3a** is again coupled with the pyramidal inversion of the two nitrogen atoms.

The problem associated with the C═C rotational transition structure can thus be recognized as 3-fold: (1) does it belong to pure singlet or triplet electronic states or to a certain mixture of these; (2) how large is the coupling of the real rotational transition with other intramolecular motions reflected by the corresponding transition mode; and (3) what is the real contribution of sulfur (and possibly other higher row donor atoms, e.g. P, compound **3e**, and Se, compounds **2c** and **3f**) atoms to the donor−acceptor structure and hence to the rotational barrier? The latter problem is directly related to the notion of C═C bond polarization or the push−pull effect as well. We find no anomalies in atom and bond populations for either C═S, **2b**, or C═Se, **2c**, acceptor groups against NH donors. Electronic structure, i.e., atom and bond populations, and geometry changes with C═C rotation in these two model molecules follow the general pattern found with first row acceptor atoms, N and O. However, with **2b** and **2c** (acceptors S and Se) there are exceptions of the push−pull pattern for first row DA pairs in the C═C NBO population,[32] which in fact indicate a single C−C and not a double C═C bond in both ground and transition structures for the internal rotation. In addition, NBO charges on C═C carbon atoms of **3c**, **3e**, and **3f** (donors P, S, and Se) are negative for both donor and acceptor ends of the double bond and corroborate the suggestion that with second and higher row donors C═C bond polarity can even be reversed, which is out of line for the suggested polarity−C═C rotation barrier relationship.[6] Additional details of the relationships between experimental barriers of dynamic NMR processes and electronic structure of model push−pull ethenes will be discussed below.

Singlet and Triplet Minima on the Corresponding Potential Energy Surfaces (PES). The suggestion of singlet − triplet intersystem crossing accompanying the C═C bond rotation would imply planar or approximately planar minima for the singlet electronic states of model molecules. The triplet minima would be expected to resemble the transition structures for internal rotation. ROHF/6-31G* conformational scans along the lowest singlet and triplet PES, however, indicate triplet minima at the perpendicular conformation only for sulfur compounds, independent of whether S participates in the donor, e.g. **2b**, or the acceptor fragment, e.g. **3c,** of the push−pull ethene, Figure 3.

The 8 × 8 MCSCF/6-31G* geometry optimization for **3c**−**f** does in fact locate approximately perpendicular stationary structures both as triplet minima and very close transition structures; see Figure 1 for **3d**. These perpendicular structures can be considered arising from the B_1 out-of-plane vibration of the corresponding planar symmetrical C_{2v} structure. A hint to the possible existence of shallow double triplet minima close to the perpendicular structures of DA ethenes is given also by their ROHF/6-31G* conformational scans; see Figures 2 and 3.

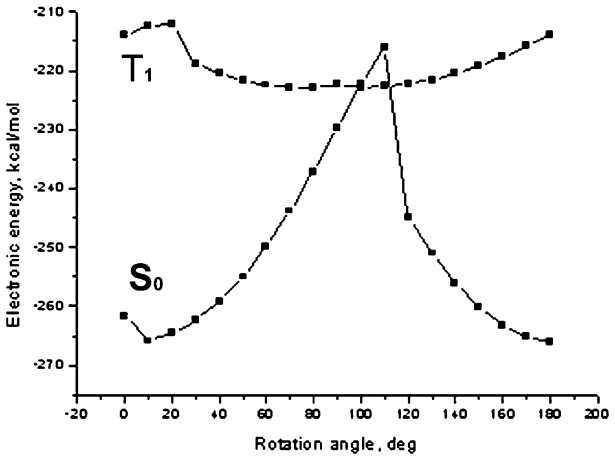

Figure 3. S_0/T_1 relaxed surface scan for **3c**, D = **S**, ROHF/6-31G*. The S_0 profile has a sharp maximum, while the T_1, a shallow double minimum zone in the region of perpendicular donor and acceptor planes within the molecule. Electronic energy is shifted by 1133 au.

SCHEME 2: Push−Pull Ethene Models with Disallowed Donor Heteroatom Inversion

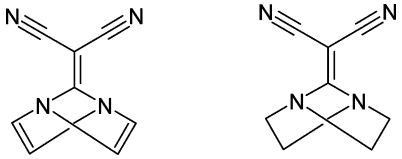

Alternatively, the A_2 vibration of the hypothetical C_{2v} structure would produce the TS−S structure in Figure 1, center, which is the result of singlet saddle point (transition structure) optimization and closely resembles the true transition structures with highly pyramidal nitrogen atoms at the MP2/6-31G* level, as shown in Figure 2 for the open model **5**.

Rotational Barriers and Electronic Structure. Optimizations of singlet structures with perpendicular planes of donor vs acceptor substituents run conveniently at the 8 × 8 MCSCF/6-31G(d) level with approximate Hessian matrixes having a single negative eigenvalue; i.e., the resulting stationary points on corresponding PES are most probably true (rotational) transition structures. In addition, geometries of these perpendicular structures are similar enough to the corresponding MP2/6-31G* true transition structure geometries. However, we are presently unable to verify the perpendicular 8 × 8 MCSCF structures as rotational transition structures by explicit calculations of vibrational frequencies at the same level of theory. Therefore, for the separation of C═C rotation and vibrational motions in a push−pull ethene we consider two rigid molecular models with the structures of **7** and **8**, Scheme 2. Like the case with models **2**−**6**, we choose to use MP2/6-31G(d) geometries and to calculate thermodynamic corrections to the total electronic energies thereof in order to obtain rotational barriers of the model molecules **7** and **8**.

Note, however, that the fixation of nitrogen atom motions in **7** and **8** also prevents the interaction of the free electron pair of N with the π-electronic system of the substituted ethene, thus reducing its polarization. This effect is clearly manifested in calculated C═C bond lengths of **7** and **8**, which are practically equal to bond lengths in an unperturbed olefin. Moreover, the MP2/6-31G* search for C═C rotational transition structures in **7** and **8** results in strong distortions and significant reduction

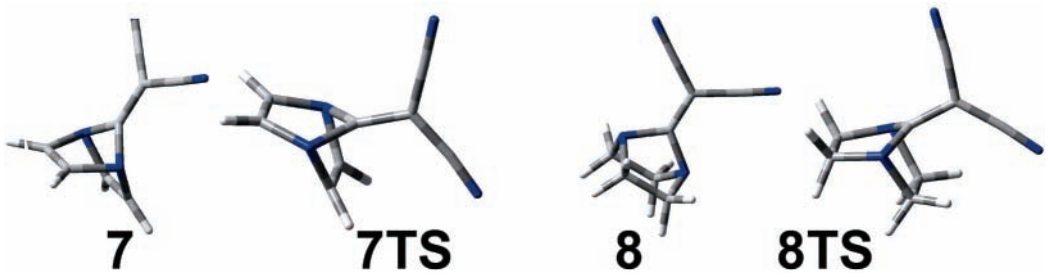

Figure 4. MP2/6-31G* stationary structures of push−pull ethenes **7** and **8**, with disallowed n−π interactions and enormous "rotation" barriers.

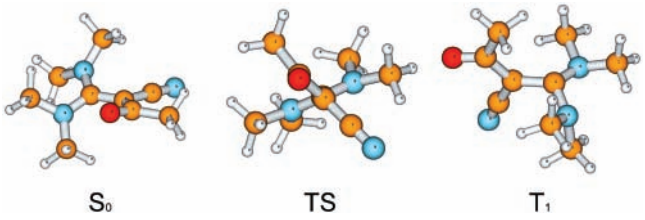

Figure 5. Local "planar" and pyramidal regions in compound **6**, 8 × 8 MCSCF/6-31G*. Nitrogen atoms are most planar in the S_0 and least planar in the almost perpendicular T_1 minima. Nitrogen atoms in the TS for the C═C "rotation" are of intermediate pyramidality.

of molecular symmetry in both models, Figure 4. The latter findings hint once again at the dominating processes in models **2**−**6**, where heteroatom lone pair−π-interactions are governing the so far modeled properties of push−pull ethenes.

Unconstrained optimizations of triplet structures of series **2**−**6** at the 8 × 8 MCSCF/6-31G* level reveal the existence of multiple minima, with various localizations of unpaired electrons. As expected, odd electrons are most frequently localized at the donor heteroatoms, rendering their configurations significantly pyramidal. Another localization of an odd electron can happen on the formally double bonded carbon atom, bearing the donor substituents. Certain minima on the triplet potential energy surfaces can also have an odd electron localized on the carbon of the electron acceptor group, CO or CN, Figure 5.

Attempts to locate S_0-S_1 conical intersections of corresponding electronic state potential energy surfaces give in most cases negative results, as do the similar attempts to find S_0-T_1 intersystem crossings. Therefore, we resort to computations of S_0-T_1 spin−orbit couplings as the characteristics of corresponding interstate interactions. These couplings are zero with O either as a donor, **2a**, or an acceptor, **3b**. In nitrogen model compounds **3a**,**d** the computed spin−orbit coupling constant is 6 cm^{-1} and again zero, respectively. Sizable spin−orbit couplings are calculated only for sulfur compounds **2b** and **3c**, a medium one of 27 cm^{-1} for the former and a really large one, 118 cm^{-1}, for the latter. The C═Se compound **2c** only has a small singlet−triplet coupling constant, 2 cm^{-1}. Calculations of open models **4**−**6** with mixed acceptor groups give small S−T couplings as well, 5, 8, and 1 cm^{-1}, respectively. Thus, the tendency of studied push−pull ethenes to involve singlet−singlet conical intersections or singlet−triplet intersystem crossings upon C═C rotation seems associated with neither molecular polarizability nor with straight polarity. At the MP2/6-31G* level, C═S and C═Se model molecules show indeed highest first polarizability α values. The thione compound **2b** also has the largest S−T spin−orbit coupling constants. With C═S and C═Se as acceptor, the model **2b** and **2c** molecules have the lowest C═C rotational barrier among their series, Table 1, at all theoretical levels. To the contrary, however, in the **3a**−**f** series, with first, second, and third row donors vs first row acceptors, the lowest C═C barriers are associated with the most polarized **3a**,**d**. The Se donor, on the other hand, brings about the largest computed S−T coupling constants, 259 cm^{-1}, for the ground rotational structure of compound **3f** and the huge 360 cm^{-1} for its apparent rotational transition structure. Compound **3e**, with the PH donor group, has the relatively low S−T coupling constants of 8 cm^{-1} for the ground rotational structure and 33 cm^{-1} for the rotational transition structure.

The importance of a multiconfigurational account for electron correlation is specifically demonstrated in the **3a**−**f** series, with the lowest barrier calculated at the 8 × 8 MCSCF/6-31G* level for the sulfur compound **3c**. Thus, no straightforward correlation is apparent between the theoretical electronic structure quantities and the C═C rotational barrier. Still, the possibility remains that a correlation between polarizabilities and C═C rotational barriers could be found with a large enough series of push−pull ethenes, as already shown with polarity and rotational barriers.[6] Such a relationship would certainly encompass very limited ranges of similar molecules inasmuch as polarizability is a global molecular characteristic, while the C═C rotational barrier is a quantity associated with a localized molecular fragment. Indeed, with a series of 25 molecules with known barriers,[6] we obtain at best only hints to the possible relationship of experimental barriers vs molecular polarizabilities. The prediction that compound **2c**, with the C═Se acceptor group, i.e., Se participating in the π-conjugation leading to high polarizability, should have a low "donor−acceptor" C_D-C_A rotational barrier, ca. 13 kcal.mol^{-1}, is still an indication that high d-orbital contribution to bonding is likely to bring low rotational barriers as well. This latter result is consistent with the low NBO population of the C_D-C_A bond with S and Se acceptors actually corresponding to a single bond, as well as with the "correct" polarity of the bond, i.e., high positive NBO charge on the donor end and negative NBO charge on the acceptor end for **2b** and **2c**. To the contrary, for weak π-donors PH, compound **3e**, and Se, compound **3f**, calculations at correlated MO levels predict large C═C rotational barriers, large NBO population of the C═C bond, low or inverted polarity, and low molecular polarizability.

To summarize, no direct relation is apparent between either rotational barriers and C═C bond polarity or barriers and D−A pairing. The only consistent finding related to electronic structures of push−pull ethenes is that increased S−T spin−orbit interaction constants, high polarity, and high polarizability meet low calculated and experimental barriers of C═C rotation in sulfur compounds, with S as either donor or acceptor.

Steric Factors and Rotational Barriers. Nonplanar equilibrium structures of push−pull ethenes[6,13] suggest that the interpretation of observed dynamic NMR intramolecular processes as C═C rotations needs certain reformulation. Inspection

of lowest vibrational frequencies of studied push−pull ethene models, Figure 2, shows that the antisymmetric out-of-plane mode involving substituents at the C═C bond is usually the first of these. Essentially the same mode in the corresponding "rotational" TS constitutes the conformational transition vector, Figure 2. However, smooth rotation of equilibrium into perpendicular structures via the planar atomic configuration is only possible with O and S as donor substituents and is hardly achievable even with NH, which forms hydrogen bonds with acceptor substituents and thus significantly modifies observed barriers.[13] Thus, while the global S_0 and T_1 minima of studied donor−acceptor ethenes are nonplanar,[10,13] formal rotations around the C═C bond are in fact coupled large-amplitude motions of the same symmetry within the surrounding molecular fragments. The first is the pyramidal inversion of donor substituents, and the second is the antisymmetric out-of-plane vibration of ethene substituents, none of these having the planar minimum due to either steric reasons in **4**−**6** or to the nonplanar minimum for a five-membered saturated heterocyclic ring pseudorotation in **2** and **3**. Specifically, with turning the acceptor part of the molecule out of the π-symmetry plane, the donor part of the molecule becomes increasingly nonplanar as well. In fact, each heteroatom, having approximately the planar sp^2 configuration in the S_0 minimum, becomes more pyramidal, i.e., closer to sp^3, in the C═C twisted configurations; see Figures 1, 2, 4, and 5, and the Supporting Information. The mentioned large-amplitude motions are significantly more pronounced for molecules without internal constraints, such as **4**−**6**. Intramolecular motions in the chosen **2** and **3** species are significantly restricted by the five-membered ring.

Molecules without internal constraints and with sizable substituents, as **6**, are nonplanar in the ground S_0 state and sterically strained enough to assume that in the best case the C═C "rotation" remains a large-amplitude out-of-plane libration. This suggestion is strongly supported by the observed coupling of the rotational transition mode with pyramidal inversion modes of heteroatom substituents, in particular involving donor atoms, as described in previous sections. Immobilization of inversion modes in model compounds **7** and **8**, indeed, brings significant increase of the C═C rotational barrier and, thus, additionally supports the suggestion that the observed dynamic NMR phenomena of push−pull ethenes are rather the result of coupling of large amplitude n-electron governed heteroatom inversion and out-of-plane vibrational modes.

Both X-ray crystallography and earlier quantum mechanical wave function and density functional theory calculations[10,13] indicate that push−pull ethenes require significant factors to favor planar structures, such as intramolecular hydrogen bonds between carbonyl oxygen atoms and, e.g. RNH−donors. To the contrary, sterically demanding substituents favor nonplanar and even perpendicular equilibrium structures.[10] Sterically demanding substituents would however simultaneously preclude full rotations around the polarized C═C bond and nevertheless leave the corresponding molecules still showing the characteristic dynamic NMR features of strongly polarized ethenes. Therefore, in our opinion these rapid NMR but slow vibrational processes should be more reliably interpreted as large-amplitude rovibrationally coupled C═C out-of-plane librations, that is, intramolecular motions sterically restricted to span only certain sectors of the complete rotations about the C═C bonds, not involving planar arrangements as stationary points on the corresponding potential energy profiles.

Acknowledgment. The work at the University of Alcalá de Henares was financed under Project BQU2003-07281 from the Spanish Ministry of Science and Technology (MCyT). J.K. thanks the Spanish Ministry of Education, Culture and Sport for financial support during his Sabbatical year at the Department of Physical Chemistry of the University of Alcalá de Henares (Madrid), Spain. Partial financial support was made available by the Bulgarian Science Fund under Grant X-1408.

Supporting Information Available: Full tables with computational results, comparisons of MP2/6-31G*, and 8 × 8 CAS SCF/6-31G* geometries of model molecules, MP2/6-31G* geometries, 8 × 8 MCSCF/6-31G* and MP2/6-31G* geometries, RHF/6-31G* orbitals of **7** and the MCSCF orbital selection, GUGA-CI distribution of CSFs in 8 × 8 MCSCF states, Mulliken and NBO populations, and NMR rotational barriers. This material is available free of charge via the Internet at http://pubs.acs.org.

References and Notes

(1) Turro, N. J. *Modern Molecular Photochemistry*; University Science Books: Sausalito, CA, 1991.

(2) Forni, A.; Destro, R. *Chem. Eur. J.* **2003**, *9*, 5528.

(3) Dwyer, T. J.; Jasien, P. G.; Kirkowski, S. M.; Buxton, C. M.; Arruda, J. M.; Mitchell, G. M. *J. Am. Chem. Soc.* **1998**, *120*, 12942. Dwyer, T. J.; Jasien, P. G. *J. Mol. Structure (THEOCHEM)* **1996**, *363*, 139.

(4) Sandström, J.; Sjöstrand, U.; Wennerbeck, I. *J. Am. Chem. Soc.* **1977**, *99*, 4526.

(5) Benassi, R.; Bertarini, C.; Taddei, F.; Kleinpeter, E. *J. Mol. Struct. (THEOCHEM)* **2001**, *541*, 101.

(6) Kleinpeter, E.; Klod, S.; Rudorf, W.-D. *J. Org. Chem.* **2004**, *69*, 4317.

(7) Benassi, R.; Bertarini, C.; Kleinpeter, E.; Taddei, F. *J. Mol. Struct. (THEOCHEM)* **2000**, *498*, 217.

(8) Denkova, P. S.; Dimitrov, V. S. Manuscript in preparation.

(9) Benassi, R.; Bertarini, C.; Hilfert, L.; Kemper, G.; Kleinpeter, E.; Spindler, J.; Taddei, F.; Thomas, S. *J. Mol. Struct.* **2000**, *520*, 273.

(10) Fischer, G.; Kleinpeter, E. *Magn. Reson. Chem.* **1991**, *29*, 204.

(11) Dimitrov, V. S.; Vassilev, N. G. *Magn. Reson. Chem.* **1995**, *33*, 739. Denkova, P. S.; Dimitrov, V. S. *Magn. Reson. Chem.* **1999**, *37*, 637.

(12) Dwyer, T. J.; Norman, J. A.; Jasien, P. G. *J. Chem. Educ.* **1998**, *75*, 1635. Aguirre, G.; Somanathan, R.; Hellberg, L. H.; Dwyer, T. J.; North, R. *Magn. Reson. Chem.* **2003**, *41*, 131.

(13) Bernhardt, P. V.; Koch, R.; Moloney, D. W. J.; Shtaiwi, M.; Wentrup, C. *J. Chem. Soc., Perkin Trans. 2* **2002**, 515.

(14) Benassi, R.; Bertarini, C.; Kleinpeter, E.; Taddei, F.; Thomas, S. *J. Mol. Struct. (THEOCHEM)* **2000**, *498*, 201.

(15) Taddei, F. *J. Mol. Struct. (THEOCHEM)* **2001**, *544*, 141.

(16) Alkorta, I.; Wentrup, C.; Elguero, J. *J. Mol. Struct. (THEOCHEM)* **2002**, *585*, 27.

(17) Rappalardo, R. R.; Marcos, E. S.; Ruiz-Lopez, M. F.; Rinaldi, D.; Rivail, J.-L. *J. Am. Chem. Soc.* **1993**, *115*, 3722. Benassi, R.; Bertarini, C.; Taddei, F.; Kleinpeter, E. *J. Mol. Struct. (THEOCHEM)* **2001**, *504*, 101.

(18) Head-Gordon, M.; Pople, J. A. *J. Phys. Chem.* **1993**, *97*, 1143.

(19) Matus, M. H.; Contreras, R.; Cedillo, A.; Galvan, M. *J. Chem. Phys.* **2003**, *119*, 4112.

(20) Schmidt, M. W.; Gordon, M. S. *Annu. Rev. Phys. Chem.* **1998**, *49*, 233−266.

(21) Brooks, B.; Schaefer, H. F. *J. Chem. Phys.* **1979**, *70*, 5092.

(22) Bernardi, F.; De, S.; Olivucci, M.; Robb, M. A. *J. Am. Chem. Soc.* **1990**, *112*, 1737. Bernardi, F.; Olivucci, M.; Robb, M. A. *Acc. Chem. Res.* **1990**, *23*, 405.

(23) Frisch, M. J.; Trucks, G. W.; Schlegel, H. B.; Scuseria, G. E.; Robb, M. A.; Cheeseman, J. R.; Montgomery, J. A., Jr.; Vreven, T.; Kudin, K. N.; Burant, J. C.; Millam, J. M.; Iyengar, S. S.; Tomasi, J.; Barone, V.; Mennucci, B.; Cossi, M.; Scalmani, G.; Rega, N.; Petersson, G. A.; Nakatsuji, H.; Hada, M.; Ehara, M.; Toyota, K.; Fukuda, R.; Hasegawa, J.; Ishida, M.; Nakajima, T.; Honda, Y.; Kitao, O.; Nakai, H.; Klene, M.; Li, X.; Knox, J. E.; Hratchian, H. P.; Cross, J. B.; Adamo, C.; Jaramillo, J.; Gomperts, R.; Stratmann, R. E.; Yazyev, O.; Austin, A. J.; Cammi, R.; Pomelli, C.; Ochterski, J. W.; Ayala, P. Y.; Morokuma, K.; Voth, G. A.; Salvador, P.; Dannenberg, J. J.; Zakrzewski, V. G.; Dapprich, S.; Daniels, A. D.; Strain, M. C.; Farkas, O.; Malick, D. K.; Rabuck, A. D.; Raghavachari, K.; Foresman, J. B.; Ortiz, J. V.; Cui, Q.; Baboul, A. G.; Clifford, S.; Cioslowski, J.; Stefanov, B. B.; Liu, G.; Liashenko, A.; Piskorz, P.; Komaromi, I.; Martin, R. L.; Fox, D. J.; Keith, T.; Al-Laham, M. A.;

Peng, C. Y.; Nanayakkara, A.; Challacombe, M.; Gill, P. M. W.; Johnson, B.; Chen, W.; Wong, M. W.; Gonzalez, C.; Pople, J. A. *Gaussian 03*, Revision B.05; Gaussian, Inc.: Wallingford, CT, 2004.

(24) Nakano, H. *J. Chem. Phys*. **1993**, *99*, 7983.

(25) GAMESS−US: Schmidt, M. W.; Baldridge, K. K.; Boatz, J. A.; Elbert, S. T.; Gordon, M. S.; Jensen, J. H.; Koseki, S.; Matsunaga, N.; Nguyen, K. A.; Su, S. J.; Windus, T. L.; Dupuis, M.; Montgomery, J. A. *J. Comput. Chem.* **1993**, *14*, 1347. Analytical second derivatives of MCSCF energy vs atomic coordinates are available as of November 2004.

(26) Hehre, W**.** J.; Radom, L.; Schleyer, P. v. R.; Pople, J. A. *Ab Initio MO Theory*; Wiley: New York, 1986.

(27) Dunning, T. H., Jr. *J. Chem. Phys*. **1989**, *90*, 1007.

(28) Fedorov, D. G.; Koseki, S.; Schmidt, M. W.; Gordon, M. S. *Int. Rev. Phys. Chem*. **2003**, *22*, 551.

(29) Furlani, T. R.; King, H. F. *J. Chem. Phys*. **1985**, *82*, 5577. King, H. F.; Furlani, T. R. *J. Comput. Chem.* **1988**, *9*, 771.

(30) MOLDEN 4.3: Schaftenaar G.; Noordik, J. H. *J. Comput.-Aided Mol. Des.* **2000**, *14*, 123.

(31) Fischer, G.; Rudorf, W.-D.; Kleinpeter, E. *Magn. Res. Chem.* **1991**, *29*, 212.

(32) Reed, A. E.; Carpenter, J. E.; Weinhold, F. *Chem. Rev.* **1988**, *88*, 899.